Available online at www.sciencedirect.com
SCIENCE DIRECT®
Thermochimica Acta 426 (2005) 191–198
thermochimica acta
www.elsevier.com/locate/tca

Phase polymorphism of $[Co(DMSO)_6](ClO_4)_2$ studied by differential scanning calorimetry☆

A Migdał-Mikuli*, E. Szostak

Department of Chemical Physics, Faculty of Chemistry, Jagiellonian University, ulica Ingardena 3, 30-060 Kraków, Poland

Received 20 April 2004; received in revised form 27 July 2004; accepted 30 July 2004
Available online 15 September 2004

Abstract

Five solid phases of $[Co(DMSO)_6](ClO_4)_2$ have been detected by differential scanning calorimetry (DSC). Specifically, the phase transitions were detected between the following solid phases: metastable KIII ↔ overcooled K0 at T_{C4} = 329 K, stable KIb → stable KIa at T_{C3} = 350 K, metastable KII ↔ overcooled K0 at T_{C2} = 363 K and stable KIa → stable K0 at T_{C1} = 377 K. The title compound melts gradually in three steps with final melting point at T_m = 495 K. From the entropy changes of the melting point and phase transitions it can be concluded that phases K0 and overcooled K0 are orientationally dynamically disordered phases. Stable phases KIa, KIb and metastable phase KIII are ordered solid phases. Metastable phase KII is probably a solid phase with a high degree of orientational dynamical disorder.

Keywords: Hexadimethylsulphoxidecobalt(II) chlorate(VII); Phase transitions; Melting point; DSC

1. Introduction

Hexadimethylsulphoxidecobalt(II) chlorate(VII) (called HCC) consists of two kinds of complex ions: $[Co((CH_3)_2SO)_6]^{2+}$ and ClO_4^-. The cation is a slightly deformed octahedron, the cobalt atom being surrounded by six oxygen atoms coming from the dimethylsulphoxide (DMSO) ligands. The DMSO ligands are built like C_{2v} pyramids. The crystal structure of HCC is unknown. However, analogous $[Cd(DMSO)_6](ClO_4)_2$ crystallises in rhombic system (space group: No 43; Fdd2; C_{2v}^{19} [1]). We have recently investigated the polymorphism of $[Cd(DMSO)_6](ClO_4)_2$ by DSC method [2] and found five solid phases. Three of them were stable and two were metastable. The high temperature phase K0 and the metastable phases KII and KIII are dynamically orientationally disordered crystals (ODDIC). The purpose of this work was to carefully examine the polymorphism of $[Co(DMSO)_6](ClO_4)_2$ at 153–530 K using differential scanning calorimetry (DSC) in order to compare it with that of the hexadimethylsulphoxidecadmium(II) chlorate(VII).

2. Experimental

2.1. Sample preparation

A few grams of $[Co(H_2O)_6](ClO_4)_2$ were dissolved while being slowly heated up in DMSO of high chemical purity [3], which was previously additionally purified by vacuum distillation at low pressure. This solution was then chilled and the precipitated crystals of HCC were filtered and washed with acetone. They were then dried in a desiccator over phosphorous pentaoxide for a few hours. After desiccation, they were put in a sealed vessel and stored in a desiccator with barium oxide as a desiccant.

To check the chemical composition of the synthesised HCC, the percentage content of cobalt ions was checked using a complexometric method, with a solution of the sodium

☆ The paper is dedicated to the memory of Doc. Dr. Hab. Jacek Mayer (1944–2003).

* Corresponding author. Tel.: +48 12 633 6377x2256; fax: +48 12 634 0515.
E-mail addresses: migdalmi@chemia.uj.edu.pl, mikuli@chemia.uj.edu.pl (A. Migdał-Mikuli).

0040-6031/$ – see front matter © 2004 Elsevier B.V. All rights reserved.
doi:10.1016/j.tca.2004.07.021

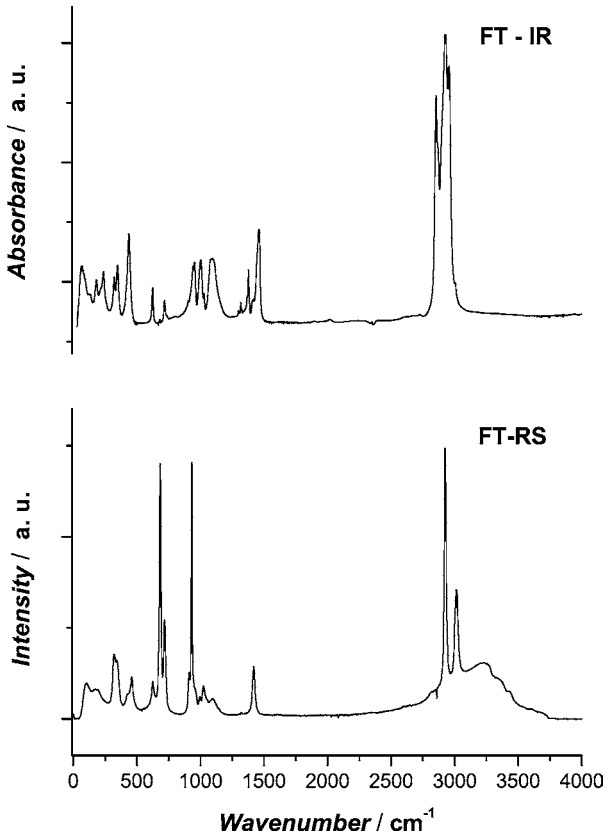

Fig. 1. Comparison of the infrared (FT-FIR and FT-MIR) and Raman (FT-RS) spectra of $[Co(DMSO)_6](ClO_4)_2$ – HCC.

salt of ethylenediaminetetraacetic acid (EDTA) as a titrant. The content of carbon and hydrogen in the DMSO ligand was determined using elementary analysis on a EURO EA 3000 apparatus. The theoretical content of cobalt equalled 8.11% and its content found by the titration analysis amounted to 7.84 ± 0.12%. For carbon atoms, the difference between the theoretical value (19.83%) and the test value (19.90 ± 0.01%) did not exceed 0.1%. For hydrogen atoms, the theoretical value was 5.00% and the test value was 4.94 ± 0.01%. Therefore, the elementary analysis of the title compound confirmed presence of the stoichiometric number of six DMSO molecules in the complex cation.

2.2. Sample characteristics

In order to further identify the title compound, its infrared absorption spectra (FT-FIR and FT-MIR) and its Raman spectrum (FT-RS) were recorded at ambient temperature. The FT-FIR and FT-MIR spectra were made using Digilab FTS-14 and EQUINOX-55 Bruker Fourier transform infrared spectrometers, respectively, with a resolution of 2 cm^{-1} The FT-FIR spectrum for powder samples, suspended in apiezon grease, was recorded. Polyethylene and silicon windows were used. The FT-MIR spectrum was recorded for a sample suspended in Nujol between the KBr pellets. The FT-RS spectrum was recorded using a Bio-Rad spectrometer with a YAG neodymium laser (λ = 1064 nm) at 10–4000 cm^{-1} with a resolution of 4 cm^{-1}. Fig. 1 presents a comparison of the infrared and Raman spectra of HCC. Table 1 contains a list of the obtained and literature data [2–7] of band frequencies and their assignments. The recorded spectra additionally identify the investigated compound as $[Co(DMSO)_6](ClO_4)_2$.

Thermal analysis of the examined compound was made in order to further verification of its composition. The differential thermal analysis (DTA) and thermogravimetric (TG) measurements were performed using a Mettler Toledo TGA/SDTA 851^e apparatus. A sample weighing 16.4300 mg was placed in a 70 μl corundum crucible. The thermogravimetric measurements were made in a flow of argon (80 ml min^{-1}) from 300 K up to 500 K at a constant heating rate of 2 K min^{-1}. The temperature was measured by a Pt–Pt/Rh thermocouple with the accuracy of ±0.5 K. Fig. 2 presents a comparison of the TG, DTG and DTA curves for HCC in the temperature range of 300–380 K. It can be seen from TG and DTG curves that during the heating the sample up to 370 K it loses only ca. 2% of its initial mass. It means that the compound practically does not change its composition, even when the sample is not hermetically closed. The endothermic peak on DTA curve has its extreme value at ca. 370 K and it

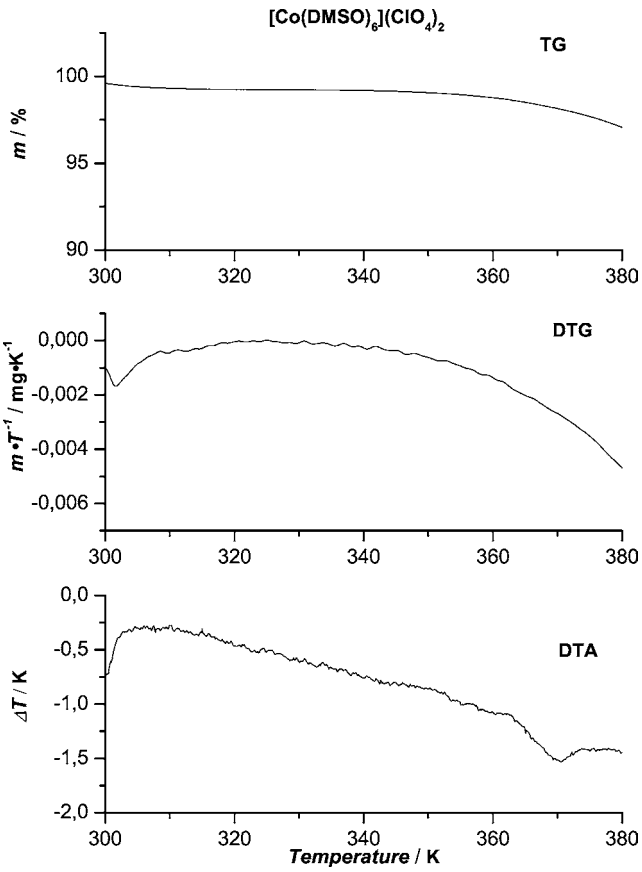

Fig. 2. TG, DTG and SDTA curves for HCC at 300–380 K.

Table 1
The list of band positions of the Raman and infrared spectra of solid $[Co(DMSO)_6](ClO_4)_2$ and $[Cd(DMSO)_6](ClO_4)_2$ at room temperature

Frequencies in cm^{-1}						Assignment
$[Co(DMSO)_6](ClO_4)_2$				$[Cd(DMSO)_6](ClO_4)_2$		M = Co and Cd
RS	IR			RS [2]	IR [2]	
This work	This work in KBr	This work	[3–7]			
		68 st[a]			54 w[a]	ν_L(lattice)
				70 sh	72 w[a]	ν_L(lattice)
102*m*		129 w[a]		116 m	106 w[a]	ν_L(lattice)
		181 m[a]			144 m[a]	ν_L(lattice)
192*w*		214 w[a]		195 w	186 m[a]	ν_d(MO)
		236 st[a]	306 sh			ν_d(MO)
320*m*		321 m[a]	322 sh	312 m	310 m[a]	δ_{as}(CSC)
344*w*		348 st[a]	344 s	341 w	336 m[a]	δ_{as}(CSO)
			356 sh			δ_s(CSO)
			382 m			ν_s(MO)
422*w*		418 m[a]	429 s	411 w	418 m[a]	ν_s(MO)
	453*w*	437 m[a]	444 s			ν_{as}(MO)
			463 sh			δ_d(OClO)*E*
459*m*	497*vw*			459 m		δ_d(OClO)*E*
625*m*	627*st*	624 m[b]	620	625 m	624 st[b]	δ_d(OClO)F_2
		662 vw[b]	661 m		669 vw[b]	ν_s(CS)
683*vst*	671*w*	680 w[b]	690 s	679 vst	677 w[b]	ν_s(CS)
718*st*	716*m*	717 m[b]		716 st	716 m[b]	ν_{as}(CS)
910*w*		902 sh[b]	887 w	910 w		$\rho(CH_3)$
932*vst*	938*sh*	936 st[b]		932 st		ν_s(ClO)A_1
			921 m		940 st[b]	$\rho(CH_3)$
961*w*	953*st*	953 st[b]	946 m	959 w	952 st[b]	$\rho(CH_3)$
996*w*		1000 st[b]		1003 w	999 st[b]	$\rho(CH_3)$
1024*m*	1021*vst*	1029 sh[b]	1012 m	1026 m	1034 sh[b]	ν_s(SO)
			1055 vs	1039 sh		ν_s(SO)
					1058 sh[b]	
1096*m*	1105*m*	1093 st[b]		1096 m	1098 vst[b]	ν_d(ClO)F_2
		1150 w[b]			1126 vst[b]	
	1299*sh*	1299 vw[b]	1306 m		1300 sh[b]	δ_s(HCH)
	1319*m*	1318 m[b]	1325 w		1319 m[b]	δ_s(HCH)
		1377 st[b]	1404 m		1377 st[b]	δ_{as}(HCH)
1420*st*	1408*m*	1412 m[b]	1416 m	1422 st	1414 sh[b]	δ_{as}(HCH)
	1435*m*	1461 vst[b]	1436 s	1432 sh	1457 vst[b]	δ_{as}(HCH)
		2885 vst[b]		2814 vw	2854 vst[b]	ν_s(CH)
		2871 sh[b]		2867 vw	2871 sh[b]	ν_s(CH)
2924*vst*	2916*w*	2928 vst[b]	2918 m	2922 vst	2921 vst[b]	ν_s(CH)
		2955 vst[b]			2959 vst[b]	ν_{as}(CH)
3015*st*	2996*w*		3000 m	3007 st		ν_{as}(CH)
3225*m*						

vw – very weak, w – weak, sh – shoulder, m – medium, st – strong, vst – very strong, br – broad.
[a] In Apiezon.
[b] In Nujol.

is related to described below phase transition at T_{C1} = 377 K. From 370 to 495 K the sample losses in two-stage process 2 DMSO molecules per formula unit.

2.3. Heat flow measurements

The DSC measurements of HCC were made using a Perkin-Elmer DSC-7 apparatus at 153–393 K for two samples airtight hermetically closed in 30 μl aluminium containers. The weights of these samples were: sample A: 8.10 mg and B: 15.05 mg. After the measurements the sample masses were exactly the same. The instrument was calibrated by means of melting points of indium and zinc for the high-temperature region, and the melting point of H_2O and solid phase transition at T_C = 234.5 K in NH_4Br for the low-temperature region. The other details of the DSC experiment were the same as published in [8].

3. Results and discussion

The temperature dependences of the difference in thermal power supplied to the two calorimeters (the so-called thermal stream or heat flow), named DSC curves, were obtained for each of two HCC samples A and B at different scanning rates and at different initial and final sample heating and cooling

Table 2
Thermodynamics parameters of the detected phase transitions (on heating) in $[Co(DMSO)_6](ClO_4)_2$ and $[Cd(DMSO)_6](ClO_4)_2$

	$[Co(DMSO)_6](ClO_4)_2$			$[Cd(DMSO)_6](ClO_4)_2$		
	T_c (K)	ΔH (kJ mol^{-1})	ΔS (J mol^{-1} K^{-1})	T_c (K)	ΔH (kJ mol^{-1})	ΔS (J mol^{-1} K^{-1})
T_m	495 ± 1	14.75 ± 0.53	29.8 ± 1.1	465 ± 1	28.10 ± 2.53	60.5 ± 5.4
T_{C1}	377 ± 1	28.03 ± 1.06	74.3 ± 2.8	376 ± 1	31.30 ± 1.05	83.2 ± 2.5
T_{C2}	363 ± 1	2.36 ± 0.22	6.4 ± 0.7	347 ± 1	6.63 ± 0.35	19.1 ± 0.9
T_{C3}	350 ± 1	2.13 ± 0.08	6.1 ± 0.2	318 ± 1	13.42 ± 0.58	42.2 ± 1.9
T_{C4}	324 ± 1	21.74 ± 0.13	67.1 ± 0.4	242 ± 1	0.64 ± 0.03	2.6 ± 0.2

conditions. Masses of the samples were chosen so as to determine whether the observed phase transition depends on the sample weight, or not. We did not notice significant differences between the results obtained for sample A and B, so we will present only the results for sample A. The thermodynamic parameters of the phase transitions are presented in Table 2, together with the results for $[Cd(DMSO)_6](ClO_4)_2$, in order to their comparison. The results of all DSC measurements are also schematically presented altogether as a temperature dependence of the free enthalpy G (Gibbs free energy) and shown in Fig. 3. As an insertion in Fig. 3 were placed the results for cadmium compound.

Samples without any "thermal history" are in a crystalline phase called KIb phase. The measurements on sample a were started by cooling the sample from room temperature (RT) to 153 K, holding it at this temperature for 1 min, then heating it up to 393 K and then cooling it again down to 153 K. DSC curves obtained on first cooling (No 1) and subsequent heating (No 2) of sample A, with a scanning rate of 20 K min, are shown in Fig. 4. As can be seen in Fig. 4, while cooling sample from RT to 153 K, no anomaly on the DSC curve was recorded. While heating this sample, being initially in the KIb phase, from 153 to 393 K, a phase transition into an intermediate phase which was named KIa can be observed above TR, namely at T_{C3} = 350 K, which is manifested in a small anomaly on the DSC curve No 2. Phase KIa next transforms into the high temperature K0 phase at T_{C1} = 377 K, which is manifested in a big anomaly on the same curve (see Fig. 4 and compare with Fig. 3).

Later, while cooling sample from 393 K with a scanning rate of 10 K min, being in the K0 phase, it undergoes a deep overcooling. As can be seen in Fig. 5 (DSC curve No 3), when the sample being cooled, the overcooled K0 (named also Kd) phase experiences a phase transition at T_{C4} = 329 K into a metastable phase, called KIII phase, which was connected with a big anomaly on the DSC curve. On further cooling, at ca. 300 K the KIII phase undergoes a spontaneous transformation partially into the metastable phase KII and partially into stable phase KIa, which is manifested in a small anomaly on the DSC curve (see Fig. 5 and compare with Fig. 3).

New heating of the sample A with a scanning rate of 10 K min gives the DSC curve No 4 presented in Fig. 5. The sample in the metastable phase KIII transforms by an endothermic process partially into the overcooled phase K0 at T_{C4} (small but sharp endothermic anomaly on the DSC curve) and at a little higher temperature the overcooled phase

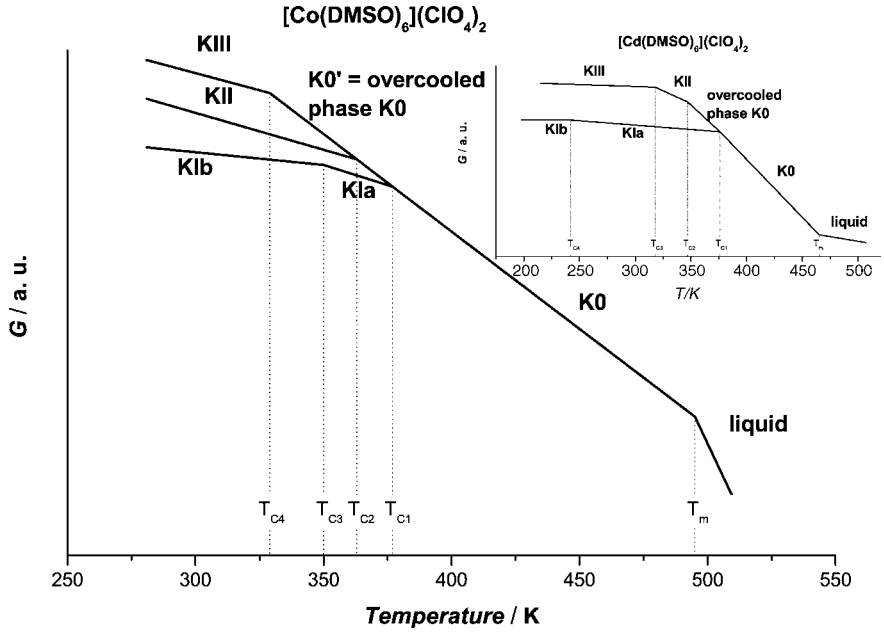

Fig. 3. Scheme of temperature dependence of the free enthalpy G for HCC. Insertion: G vs. T for $[Cd(DMSO)_6](ClO_4)_2$ (HC).

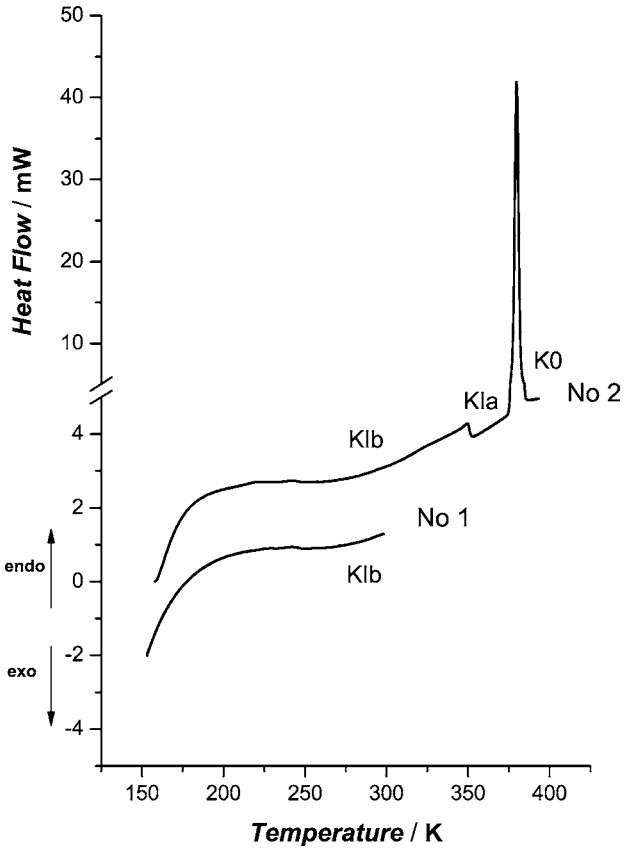

Fig. 4. Differential scanning calorimetry (DSC) curves obtained during cooling from RT to 153 K (curve No 1) and during heating at 153–393 K (curve No 2) of HCC with a scanning rate of 20 K min.

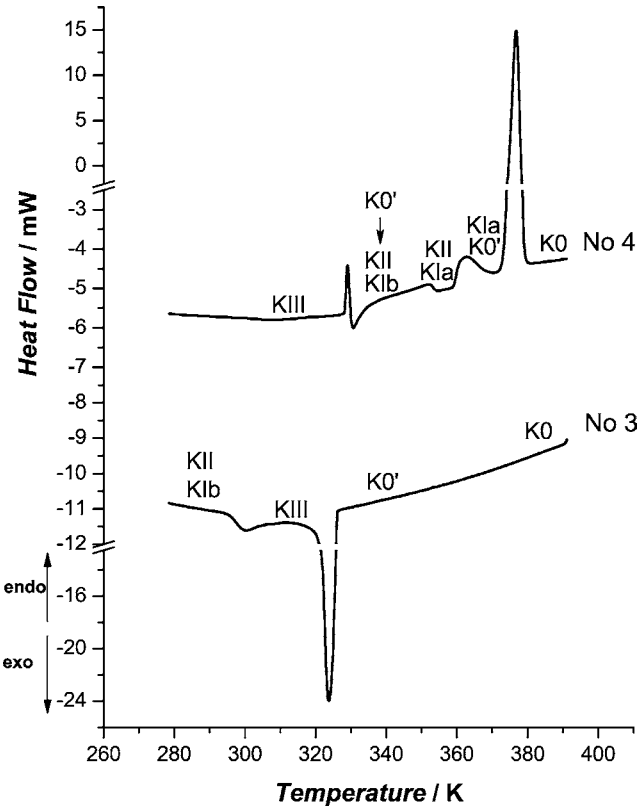

Fig. 5. DSC curves obtained during cooling from 393 to 273 K (curve No 3) and during heating at 273–383 K (curve No 4) of HCC with a scanning rate of 10 K min.

K0 converts at the exothermic process to the metastable phase KII and to the stable phase KIb (sharp exothermic anomaly). We believe that this process is similar to crystallisation of a new phase [9]. When the heating of sample is continued, the phase transition occurs from phases KIb to KIa at T_{C3} (very small and broad endothermic anomaly) and, at a slightly higher temperature, phase KII converts exothermically to the phase KIa (broad exothermic anomaly), and then the rest of the phase KII transforms into the overcooled phase K0 at T_{C2} (small and broad endothermic anomaly). In the end, the stable phase KIa also endothermically converts at T_{C1} do the stable phase K0 (very big anomaly on the DSC curve). All these transitions can also be identified on the scheme presented in Fig. 3.

However, the second new cooling of the sample a with a scanning rate of 5 K min gives a somewhat different picture of the phase transformation, which can be seen on the DSC curves presented in Fig. 6. While the sample being in the K0 phase is cooled from 393 K it becomes an overcooled but not as deep as before. As shown in Fig. 6 (DSC curve No 5), while being cooled the overcooled K0 phase, it converts partially into metastable phase KII and partially into stable phase KIa, what is connected with a big and wide anomaly on the DSC curve at ca. 352 K. On further cooling the KII phase, at ca. 340 K, it undergoes a spontaneous conversion into the phase KIb, which is manifested in a very small and broad anomaly.

When the same sample is heated up, the phase transition occurs from KIb to KIa at T_{C3} (very small and broad endothermic anomaly). Later, the rest of the phase KII transforms into the overcooled phase K0 at T_{C2} (small and broad endothermic anomaly). In the end, the stable phase KIa also endothermically converts at T_{C1} into the stable phase K0 (very big anomaly on the DSC curve). It should be stressed that on the DSC curve No 6 there is no anomaly connected with the T_{C4} phase transition, what additionally proves the presence of the metastable phase KII. All these transitions can also be identified on the scheme presented in Fig. 3.

Next, the third new cooling of the sample a with a scanning rate of 5 K min gives a more similar phase transformation picture to that which was presented in Fig. 4. It can be seen on the DSC curves presented in Fig. 7. While cooling sample A from 383 K, being in the K0 phase, it becomes deeply overcooled. As shown in Fig. 7 (DSC curve No 7), during the cooling process, the overcooled K0 phase, in a spontaneous way, partially turns into metastable phase KII, what is connected with a very weak and very broad anomaly on the DSC curve at ca. 335 K. On further cooling, the rest of the K0 phase is converted at T_{C4} into the metastable phase KIII, which is manifested in a very big anomaly.

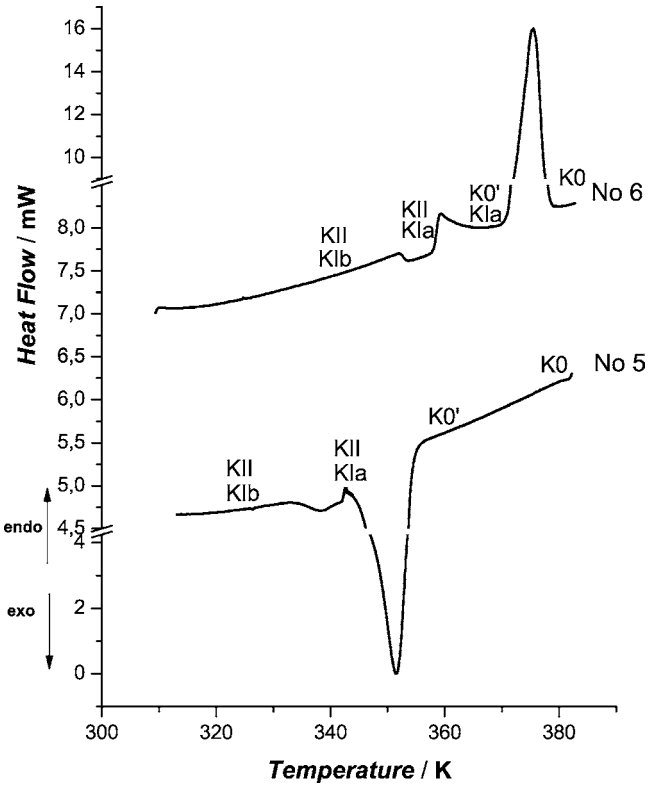

Fig. 6. DSC curves obtained during cooling from 383 to 313 K (curve No 5) and during heating at 313–383 K (curve No 6) of HCC with a scanning rate of 5 K min.

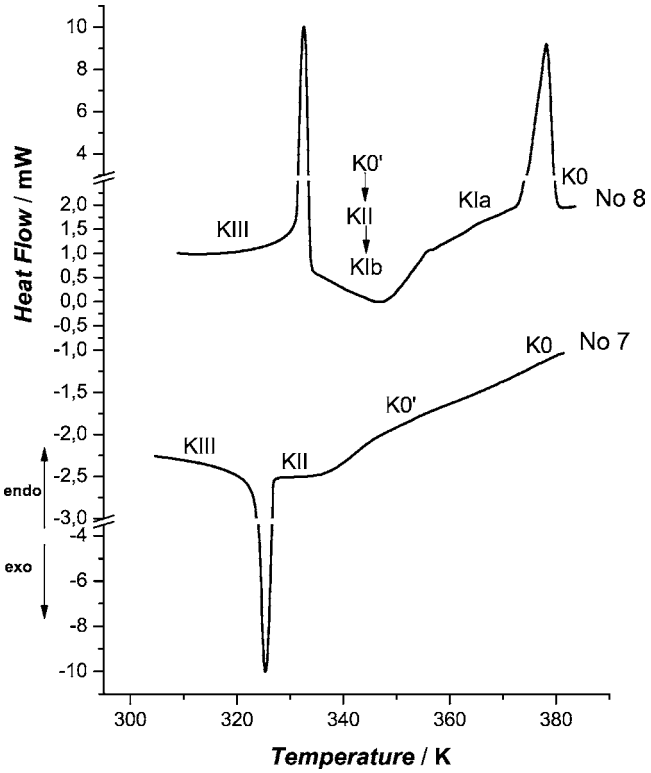

Fig. 7. DSC curves obtained during cooling from 383 to 305 K (curve No 7) and during heating at 305–383 K (curve No 6) of HCC with a scanning rate of 5 K min.

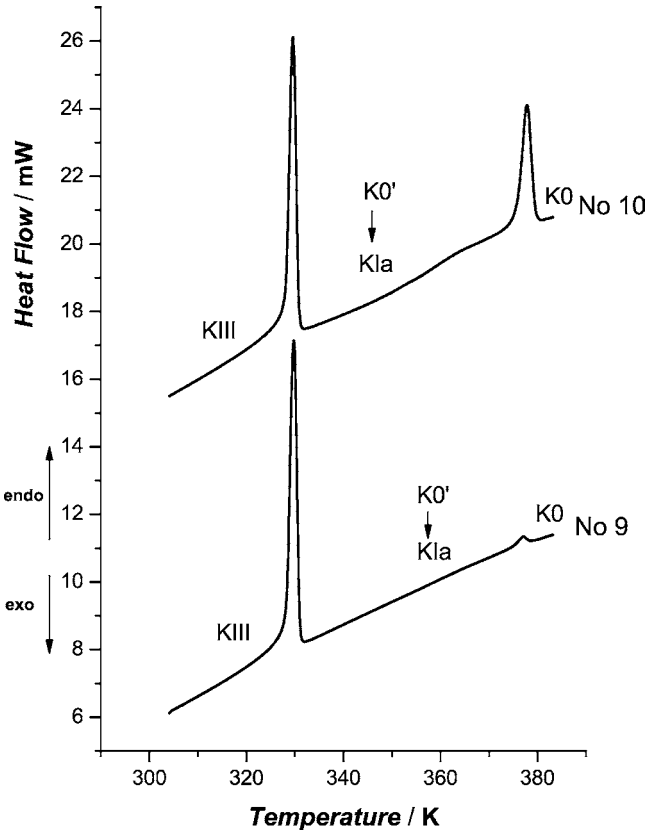

Fig. 8. Comparison of the DSC curves registered during heating from 305 to 383 K with a scanning rate of 5 K min at two different conditions of measurements.

The heating of this sample stimulates the phase transition from metastable phase KIII to overcooled phase K0 at T_{C4} (sharp endothermic anomaly on the DSC curve No 8 in Fig. 7) and then the rest of the KIII converts into the KII and KIb (small and broad exothermic anomaly at ca. 345 K). Later, there is a very small anomaly connected with the phase transition from KIb to KIa at T_{C3}. In the end, the stable phase KIb endothermically converts at T_{C1} into the stable phase K0 (sharp anomaly on the DSC curve). These transformations could also be identified on the scheme presented in Fig. 3.

In order to better clarify the metastable character of phases KII and KIII, in Fig. 8 we have compared two DSC curves registered at two different measurements. On the DSC curve No 9 we can see one big anomaly at T_{C4} connected with the phase transition: metastable phase KIII → overcooled phase K0 and only very small anomaly at T_{C1} connected with the phase transition: phase KIa → phase K0. On the curve No 10, however, because of the existence of the partial conversion from overcooled phase K0 to phase KIa, what we can see on DSC curve as a broad exothermic bump, we can also observe the distinct anomaly connected with the phase transition: stable phase KIa → stable phase K0.

It is not possible to determine the nature of the observed phases only on the basis of DSC measurements. The mea-

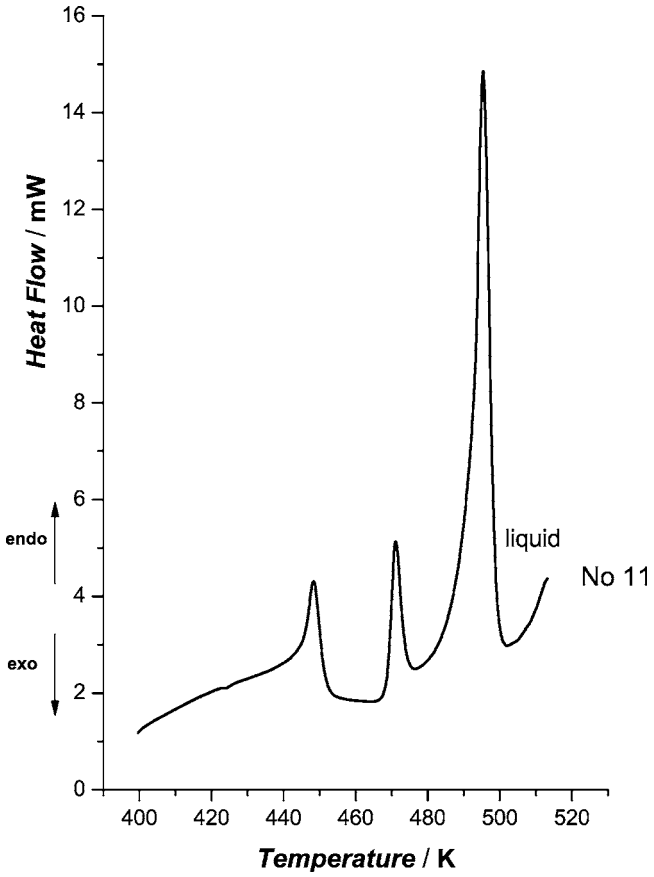

Fig. 9. DSC curve obtained in the temperature range of 400–515 K during heating of HCC with a scanning rate of 25 K min.

surements by complementary methods like for example X-ray diffraction are in progress. However, using a microscope it was observed that all the five detected phases were solid phases. Moreover, it was concluded from the change of the entropy of transitions ΔS (see Table 2) that phases K0 and overcooled K0 are more likely to be orientationally dynamically disordered crystals, the so-called "ODIC" or "ODDIC". The stochastic reorientations of the CH_3 groups, ClO_4^- anions and complex cations are present with reorientational correlation times of the order from 10^{-12} across 10^{-11} to 10^{-7} s, respectively. The $\Delta S_m = 29.8\,J\,K^{-1}\,mol^{-1}$ connected with the melting is very low but rather does not fulfil the Timmermans criterion [10] for plastic crystals. It is very probable that also the phase KII is the one of a high degree of rotational disorder too, because of the low values of ΔS for T_{C2} phase transition ($6.4\,J\,K^{-1}\,mol^{-1}$). Phases KIa, KIb and KIII are more and less ordered ones (very big values of ΔS connected with KIII ↔ K0 and KIa ↔ K0 phase transitions at T_{C4} and T_{C1}, respectively, and small value of ΔS connected with KIb ↔ KIa phase transition at T_{C3} – see Table 2.

While heating up the sample above temperature 380 K, it melts in three-stage process, first at 400 K, then at 450 K, and finally melts completely with $\Delta H_m = 14.75\,kJ\,mol^{-1}$ at T_m = 495 K. Because the title compound start to loose its DMSO ligands just above 370 K, and due to its multistage character, it is interesting to determine this decomposition as connected with the three-stage melting process, which can also be understood as the dissolution of the sample in DMSO. A DSC curve showing the anomalies resulting from the three-stage melting process of the title compound is shown in Fig. 9. Two-stage meting process connected with a partial dehydratation of the sample was observed by us in $[Ni(H_2O)_6](NO_3)_2$ [11].

Polymorphism of the title compound (HCC) described above is very similar to that of $[Cd(DMSO)_6](ClO_4)_2$ (called HC) [2] (see also Fig. 3 and Table 2). The phase transition parameters are also similar. However, the most important difference is following: in the HCC the phase transition: metastable phase KIII ↔ overcooled phase K0 at T_{C4} is at lower temperature than the phase transition between the stable phases KIa ↔ KIb at T_{C3}, whereas in the HC the phase transition: metastable phase KIII ↔ metastable phase KII at T_{C3} is at higher temperature than phase transition between the stable phases: KIa ↔ KIb at T_{C4} (see Table 2).

4. Conclusions

1. The thermodynamic parameters for the following phase transitions of HCC have been determined:
   - reversible phase transition: metastable KIII ↔ overcooled K0 at T_{C4} = 329 K.
   - irreversible phase transition: stable KIb ↔ stable KIa at T_{C3} = 350 K.
   - reversible phase transition: metastable KII ↔ overcooled K0 at T_{C2} = 363 K.
   - irreversible phase transition: KIa → K0 at T_{C1} = 377 K.
   - melting of the crystals at T_m = 495 K.
2. It can be concluded from the small values of entropy change of the melting that phases K0 and overcooled K0 are more likely to be so-called "orientationally dynamically disordered crystals" (ODDIC). Probably the metastable phase KII is the one of a high degree of rotational disorder too, because of the low values of ΔS for T_{C2} phase transition. Phases KIa, KIb and KIII are more and less ordered phases.

Acknowledgements

Our thanks are due to Dr. Hab. E. Mikuli from the Faculty of Chemistry, Jagiellonian University, for stimulating the discussion. We are also grateful to J. Ściesiński M.Sc and Dr. Hab. E. Ściesińska from H. Niewodniczański Institute of Nuclear Physics in Kraków for the FT-FIR spectrum and to Dr. A. Wesełucha-Birczyńska from the Regional Laboratory of Physicochemical Analysis and Structural Research in Kraków for the FT-RS spectrum.

References

[1] M. Sandström, Acta Chem. Scand. A 32 (1978) 519.
[2] A. Migdal-Mikuli, E. Mikuli, E. Szostak, J. Serwońska, Z. Naturforsch. 58a (2003) 341.
[3] J. Selbin, W.E. Bull, L.H. Holmes Jr., J. Inorg. Nucl. Chem. 16 (1961) 219.
[4] F.A. Cotton, R. Francis, W.D. Horrocks Jr., J. Phys. Chem. 64 (1960) 1534.
[5] M. Sandström, I. Persson, St. Ahrland, Acta Chem. Scand. A 32 (1978) 607.
[6] J.E. Connet, J.A. Creighton, J.H.S. Green, W. Kynaston, Spectrochim. Acta 22 (1966) 1859.
[7] Raman IR Atlas, Verlag Chemie GmbH, Weinheim, Bergstr., 1974.
[8] E. Mikuli, A. Migdał-Mikuli, J. Mayer, J. Therm. Anal. 54 (1998) 93.
[9] Y. Mnyukh, Fundamentals of Solid-State Phase Transitions, Ferromagnetism and Ferroelectricity, 1st Books Library, 2001.
[10] J. Timmermans, J. Phys. Chem. Solids 18 (1961) 1.
[11] E. Mikuli, A. Migdal-Mikuli, R. Chyży, B. Grad, R. Dziembaj, Thermochim. Acta 370 (2001) 65.